

OPTICAL ELECTRON BEAM DIAGNOSTICS FOR RELATIVISTIC ELECTRON COOLING DEVICES

T. Weilbach, Helmholtz-Institut Mainz, Germany,
 K. Aulenbacher, KPH Mainz, Germany
 J. Dietrich, FZJ, Germany

Abstract

For the cooling of proton and ion beams a well established overlap between cooling beam and circulating beam is needed. The new relativistic electron cooling devices, like the one proposed for the High Energy Storage Ring (HESR) at FAIR, have special demands on the diagnostics which can be used to characterize the cooling beam. Due to high voltage breakdowns they only allow a very small beam loss so non-invasive beam diagnostic methods are necessary. A system based on beam induced fluorescence (BIF) was installed at the 100 keV test setup at the Mainzer Mikrotron (MAMI). First results of the measured photon yield as a function of beam current and residual gas pressure will be presented. In addition a Thomson scattering experiment is planned at the same test setup. This method enables the measurement of other observables of the cooling beam like the electron beam energy or the electron temperature. The design of the experiment as well as the challenges will be discussed.

INTRODUCTION

The cooling beam and the cooled beam have to overlap and propagate with the same velocity to ensure a small cooling time. This matching is done by optimizing the H^0 -signal. In this case the protons of the cooled beam are recombining with the electrons of the cooling beam. The resulting Hydrogen Atoms are neutral they are not deflected by magnetic fields and can be detected after the next bending magnet. This technique is only applicable for protons and positive ions. For the cooling of antiprotons as it is planned in the (HESR) [1] there is no H^0 -signal which could indicate a good cooling rate. Because of this special beam diagnostics of the cooling beam are necessary. The diagnostic has to be non destructive because of the high beam power. It should also not affect the magnetic field flatness of the solenoids inside the cooling section.

There are already several non destructive beam diagnostic methods established. They are used in different accelerators like a scintillation profile monitor [2], [3] or the Laser wire scanner at the synchrotron source PETRA III [4]. These methods can be adapted for the use in relativistic electron cooling devices.

BEAM INDUCED FLUORESCENCE

For protons and ions beam profile measurement based on beam induced fluorescence is a common technique [5]. The idea is to image the fluorescing residual gas on a photo Electron cooling

detector with a spatial resolution as shown in Fig. 1. There are different types of detectors available, like multi channel plates (MCP), multichannel photo multiplier or intensified ccd (ICCD) cameras.

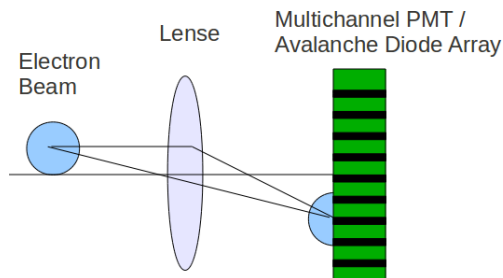


Figure 1: Principle of scintillation profile monitor

The production of the scintillation light depends on the residual gas pressure, the beam current and the composition of the residual gas. Different gases show different excitation spectra and consequential have different fluorescence spectra. But they are also differing in the intensity of the scintillation light.

For electrons and protons with the same velocity the ionization energy loss is very similar. They amount to $4.4 \text{ MeVcm}^2/\text{g}$ and $4.3 \text{ MeVcm}^2/\text{g}$ respectively for $\beta = 0.55$ in N_2 . This should lead to a corresponding light output. From the energy loss and the photo production coefficient from [6] we can therefore estimate the fluorescence rates for electrons in nitrogen gas. For our detection device which has a solid angle $\Omega = 3.1 \cdot 10^{-2} \text{ sr}$ and a detector efficiency of 0.3 we expect a count rate of 10^4 Hz/cm of longitudinal beam extension at a pressure of 10^{-6} mbar and a $100 \mu\text{A}$ beam.

To test this assumption a special vacuum chamber has been designed (Fig. 2) and has been installed at the polarized test source (PKAT) [7] at the Mainzer Mikrotron (MAMI). In this source a NEA-GaAs [8] photo cathode is used which requires 10^{-11} mbar for stable operation. Therefore this chamber together with additional turbo molecular pumps acts as a differential pumping stage. This allows local pressure bumps up to 10^{-5} mbar while maintaining the UHV condition at the cathode. The main purpose of this experiment is to gain understanding of the different background sources which degrade the signal to noise ratio for the optical beam diagnostics.

The chamber is equipped with a silica window which is transparent down to 200 nm. This allows to image the transverse beam profile by transmitting the UV parts of the spectral lines of N_2 . With the leak valve the residual gas

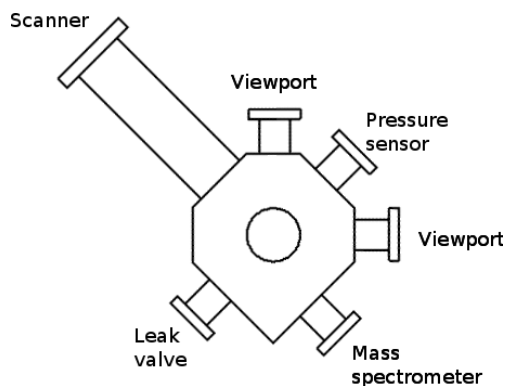


Figure 2: Vacuum chamber for beam induced fluorescence studies. The electron beam goes into the plane of the paper

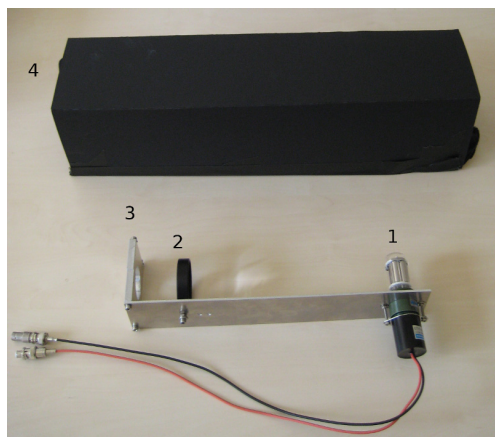


Figure 3: Imaging system consisting of PMT (1), Lens (2) and mounting system (3). Above the shielding against ambient light (4)

pressure can be changed. The pressure sensor monitors the vacuum condition. A mass spectrometer detects the partial gas pressure and enables the analysis of the photon yield of different scintillation gases.

As an imaging system for the fluorescence light a fused silica lens (wavelength range 185-2100nm) with a focal length of 12 cm is used. The distance between the electron beam and the lens is 24 cm the same as between the lens and the detector. A photomultiplier tube (PMT) with a minimal wavelength of 160 nm is used as a detector. The Fig. 3 shows the lens, the PMT and the mounting system which is used to attach the imaging system to the vacuum chamber. This whole system is shielded against light emitted by several sources (e.g. LED) in the lab.

During the first measurement a quite high background, which depended on the residual gas pressure, was observed. This background was caused by the pressure sensor. Different residual gas pressures were established with different settings of the leak valve. The leak valve was connected to a N_2 containing gas bottle. If the gas pressure was stable the pressure sensor was switched off to minimize the background for the measurement of the BIF. After that the

Electron cooling

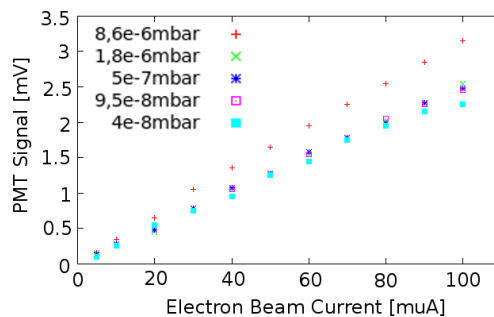


Figure 4: Beam induced fluorescence intensity against electron beam current at different residual gas pressures. The linear dependence on the beam current is clearly visible but the identical curves for pressures below 10^{-6} mbar indicate a background

pressure sensor was switched on to check if the pressure had changed. If the pressure had changed a mean value of the pressure before and after the measurement was evaluated. During the whole measurement the transmission of the electron beam was monitored with two digital volt meters (DVM). One was measuring the emitted beam current of the cathode the other was used to monitor the Faraday cup where the beam was dumped.

The PMT signal was measured against the electron beam current at different residual gas pressures. These measurements are shown in Fig. 4.

One can see clearly the linear dependence on the PMT signal of the beam current. This indicates that the signal is really produced by the electron beam. Furthermore the BIF signal of about 1 mV of a 100 keV electron beam at $8.6 \cdot 10^{-6}$ mbar (see below) corresponds to a PMT current of 10 nA. With a gain of 10^7 and a width of 8 mm of the photo multiplier this equates to $6 \cdot 10^3$ electrons per second emitted by the PMT cathode. This is a factor of 10 less than the estimated event rate mentioned above. This might be caused by uncertainties in the geometrical alignment, the PMT gain and the residual gas pressure of nitrogen. An investigation and an optimization of these uncertainties is foreseen for the future.

The more or less identical curves for pressures below 10^{-6} mbar indicate a beam induced background which is not caused by fluorescence. This might be x-rays produced in the Faraday cup or other light producing effects inside the beam pipe. Based on this assumption the background signal is 2.4 mV and the beam induced fluorescence signal (at $8.6 \cdot 10^{-6}$ mbar) is 3.2 mV. The signal to noise ratio then evaluates to 1/4.

For the future our main goal is to increase the signal to noise ratio by background reduction. This can be done with filters which are only transparent for the spectral lines of the nitrogen and by shielding the Faraday cup to get rid of the produced x-rays. A good understanding of the background is not only important for the BIF method but also for the Thomson scattering because this technique suffers from even lower counting rates.

THOMSON SCATTERING

Theory

Thomson scattering describes elastic scattering of a photon on a free electron. It is the low energy limit of the Compton scattering process. Figure 5 shows a schematic view of Thomson scattering.

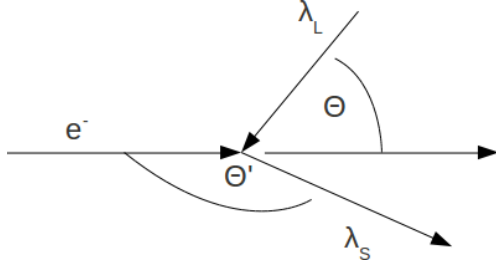


Figure 5: Thomson scattering scheme

A photon λ_L hits the electron beam under an angle Θ and is scattered under the scattering angle Θ' . The scattered photon λ_S gains energy due to the Doppler shift. The wavelength of the scattered photon as a function of the angle between incident photon and electron and the angle between scattered photon and electron can be evaluated with

$$\lambda_S = \lambda_L \frac{(1 + \beta \cos \Theta')}{(1 + \beta \cos \Theta)} \quad (1)$$

where β is the electron velocity in units of the speed of light. The scattering process is determined by the Thomson cross section

$$\frac{d\sigma}{d\Omega} = \frac{1}{2} r_e^2 (1 + \cos^2 \Theta') \quad (2)$$

with r_e = classical electron radius. The event rates i.e. how many photons are scattered can be calculated with the following equation

$$R = \frac{1}{2} r_e^2 (1 + \cos^2 \Theta') N_L n_e \epsilon \Delta\Omega l \frac{(1 + \beta \cos \Theta)}{(1 + \beta \cos \Theta')^\gamma} \quad (3)$$

with N_L = Number of incident photons per Joule, n_e = Electron density, ϵ = Detector system efficiency, $\Delta\Omega$ = Detector solid angle, l = Interaction length, $\frac{(1 + \beta \cos \Theta)}{(1 + \beta \cos \Theta')^\gamma}$ = factor results from Lorentz transformation.

Beam Diagnostics

In 1987/1988 a pioneer experiment demonstrated the feasibility of Thomson scattering for our purpose [9], [10]. At that time, however, the signal to noise ratio suffered from the low power and repetition rate of the Laser system. We revisit this approach in the light of the enormous developments in Laser technology since that time. The presented setup uses the following angles $\Theta = 90^\circ$ and $\Theta' = 180^\circ$ like a Laser wire scanner. In this case the rate of the scattered Electron cooling

photons only depends on the electron density in the electron beam. By moving the Laser beam through the electron beam a profile measurement can be done. Due to the low cross section, mostly dominated by the classical electron radius squared, the necessary Laser power is very high and it is only reasonable for high electron densities. In Tab. 1 the event rates for different setups are shown. For the calculation a 100 W Laser system and an electron beam current of 1 A and a diameter of 3 cm was chosen. The detector system efficiency $\epsilon = 0.2$ and solid angle $\Delta\Omega = 100 \text{msr}$.

Table 1: Scattering Rate for Different Cooling Devices

Electron Energy	λ_L	λ_S	Event Rate
100 keV (PKAT)	1.06 μm	475 nm	100 s^{-1}
2 MeV (COSY)	10.6 μm	220 nm	$6.5 \cdot 10^3 \text{s}^{-1}$
4.5 MeV (HESR)	10.6 μm	50 nm	$1.3 \cdot 10^4 \text{s}^{-1}$
8 MeV (ENC)	10.6 μm	20 nm	$2 \cdot 10^4 \text{s}^{-1}$

Like the BIF measurements, the Thomson scattering experiment will also be done at the PKAT. As seen in Tab. 2 the gun is capable of delivering peak currents of 60 mA with a diameter of 2 mm so the electron density is the same as in a cooling device with 2 A and 3 cm. To perform this experiment we use the setup shown in Fig. 6. This enables a detection of the scattered photons in forward direction while the electrons are bend by 270° which suppresses the background generated from fluorescent light in the beam dump.

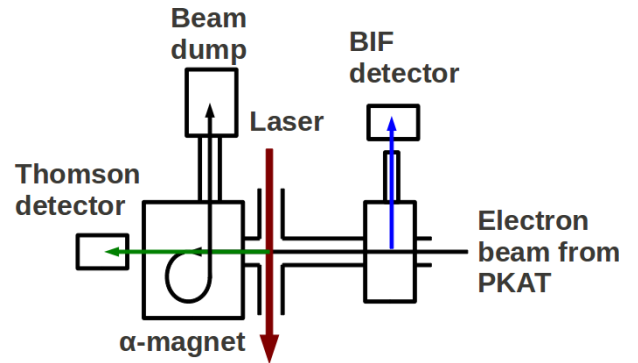


Figure 6: Schematic view of the future diagnostic setup at the PKAT

Table 2: PKAT Parameter Setup

Electron Energy	100 keV
DC current	200 μA
Beam diameter	2 mm
Peak current (pulsed)	60 mA
Pulse duration	10 ns
Rep. rate	50 Hz

An other advantage of the Thomson scattering method is the possibility to measure the electron energy. This can

be done in with the same setup which is used for the beam profile measurement. In this case a frequency analysis of the scattered photons is needed instead of the scattering rate. This can e.g. be done with a Fabry-Perot interferometer at an virtual arbitrary accuracy. Since Eq. 1 establishes a well defined relation between the angle and the velocity (i.e. the energy) the error in energy determination is mainly limited by the accuracy of the angle measurement.

This can be very interesting for the cooling of antiprotons. Because of the missing H^0 -signal an energy matching of both beams which is needed for an efficient cooling process is more difficult. With a good energy measurement the adjustment of the electron beam can be done faster and in a more efficient way.

Challenges

As mentioned above one of the challenges with Thomson scattering is the very low cross section. Because of that very high laser photon fluxes and laser powers are needed. These high power Laser beams have to be transported and focused to the interaction point without significant losses to get high signal rates and avoid a damaging of parts of the beam line. For the beam profile measurements with Thomson scattering the acquisition of a Laser system with the following specifications is planned.

Table 3: Laser System Specifications

Wavelength	1064 nm
Beam diameter	100 μm
Pulse power	2 J
Pulse duration	20 ns
Rep. rate	50 Hz

The timing between electron and Laser beam is essential for this experiment. One possibility to solve the timing problem is shown in Fig. 7. A fraction of the Laser pulse will be frequency doubled send to the photo cathode of the PKAT while the main part of the pulse is delayed. The Laser pulse has to be delayed for the time it takes the electron bunch to travel from the cathode to the interaction point. There both beams collide under an angle of 90° . The Thomson scattered photons are detected behind the α -magnet which bends the electrons by 270° . Mirrors in the Laser beam line allow a transverse shift of the Laser beam and a transverse scanning of the electron beam. The number of scattered photons is proportional to the electron density of the electron beam. If one assumes a Gaussian profile of the electron beam a Gaussian fit to the intensity of the scattered photons as a function of the displacement of the Laser provides the transversal beam profile.

Because of the low scattering rates all kind of background has to be avoided. This includes beam induced fluorescence as well as electron beam loss at the wall of the vacuum chamber or radiation emitted by the beam dump. To decrease the background the photo detector can be syn-

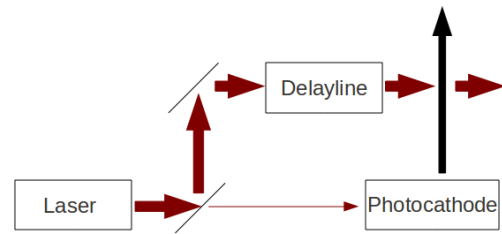


Figure 7: Laser system setup

chronized to the Laser pulses.

OUTLOOK

We are planning further investigations of the BIF method concerning a further background reduction by using spectral filters and shielding of the Faraday cup. It is also planned to use a detection system with a spatial resolution e.g. a ICCD camera.

For the Thomson scattering further modifications at the PKAT beam line are in preparation and the acquisition of an adequate Laser system is planned for 2011.

REFERENCES

- [1] T. Bergmark et al., "Status of the HESR Electron Cooler Design Work", TUPSL067, Proceedings of EPAC 2006, Edinburgh, Scotland.
- [2] C. Boehme et al., "Gas Scintillation Beam Profile Monitor at COSY Jlich", TUPSM005, Proceedings of BIW 2010, Santa Fe, New Mexico USA.
- [3] F. Becker et al., "Beam Induced Fluorescence Monitor-Spectroscopy in Nitrogen, Helium, Argon, Krypton, and Xenon Gas", TUPSM020, Proceedings of BIW 2010, Santa Fe, New Mexico USA.
- [4] M.T. Price et al., "Beam Profile Measurements with the 2-D Laser-Wire Scanner at PETRA", FRPMN094, Proceedings of PAC 2007, Albuquerque, New Mexico USA.
- [5] F. Becker, "Beam Induced Fluorescence Monitors", WEOD01, Proceedings of DIPAC 2011, Hamburg, Germany.
- [6] M.A. Plum et al., Nucl. Instr. Meth. A 492 (2002), p. 74.
- [7] P. Hartmann: "Aufbau einer gepulsten Quelle polarisierter Elektronen", Dissertation 1997, JGU Mainz, Germany
- [8] D.T. Pierce et al., Appl. Phys. Lett. 26 (1975) 670.
- [9] C. Habfast et al., "Measurement of Laser Light Thomson-Scattered from a Cooling Electron Beam", Appl. Phys. B 44, 87-92 (1987).
- [10] J. Berger et al.: Thomson Scattering of Laser Light from a Relativistic Electron Beam, Physica Scripta. Vol. T22, 296-299, 1988.